AJNR

Comparison of spin-echo MR pulse sequences for imaging of the brain.

F Fellner, C Fellner, P Held and R Schmitt

AJNR Am J Neuroradiol 1997, 18 (9) 1617-1625
http://www.ajnr.org/content/18/9/1617

Comparison of Spin-Echo MR Pulse Sequences for Imaging of the Brain

Franz Fellner, Claudia Fellner, Paul Held, and Rainer Schmitt

PURPOSE: To determine the value of the gradient- and spin-echo (GRASE) technique as compared with the fast spin-echo and conventional spin-echo techniques in MR imaging of the brain. **METHODS:** Sixty-six patients with ischemic and neoplastic brain lesions were examined with T2-weighted spin-echo, fast spin-echo, and GRASE sequences. Three independent observers evaluated the contrast characteristics of anatomic and pathologic structures and of artifacts. Quantitative image analysis included region-of-interest measurements of anatomic structures and lesions. **RESULTS:** The contrast of anatomic structures was superior in images obtained with conventional and fast spin-echo techniques as compared with those obtained with the GRASE technique. Extended lesions, such as tumors and territorial infarcts, were identified equally with all techniques. For delineation of small ischemic lesions, GRASE was slightly inferior to fast and conventional spin-echo sequences. Flow artifacts were considerably reduced with fast spin-echo and GRASE sequences. Chemical-shift artifacts were significantly reduced, but ringing artifacts were more pronounced with GRASE. **CONCLUSION:** Fast spin-echo remains the standard technique in MR imaging of the brain. However, GRASE might be useful in special cases, such as with uncooperative patients whose conventional or fast spin-echo images show severe motion artifacts.

Index terms: Brain, magnetic resonance; Magnetic resonance, comparative studies; Magnetic resonance, technique

AJNR Am J Neuroradiol 18:1617–1625, October 1997

The clinical utility of the fast spin-echo technique in routine magnetic resonance (MR) imaging of the brain has been well documented (1–8). The overall image quality of fast spin-echo sequences is similar to that of conventional spin-echo sequences. For special techniques, such as high-resolution examinations (9), image quality obtained with rapid spin-echo imaging is considered even better, since short measurement times allow more acquisitions, thereby significantly improving the signal-to-noise ratio (S/N).

A more recent approach to fast MR imaging is the gradient- and spin-echo (GRASE) technique (10–13). In contrast to fast spin-echo, GRASE sequences additionally use gradient echoes surrounding the different spin echoes with tight echo spacing, thus leading to a further reduction in measurement time. Early clinical experiences with GRASE were somewhat disappointing (14, 15) owing to heavily T2-weighted contrast behavior and pronounced blurring.

The aim of our study was to determine the value of an improved GRASE sequence relative to the fast and conventional spin-echo techniques in routine MR imaging of the brain. Patients with brain tumors and large infarctions were included to determine whether the GRASE sequence could provide similar information as that supplied by the fast and conventional spin-echo sequences. Additionally, patients with very small brain lesions (pre-

Received November 27, 1996; accepted after revision April 1, 1997.

From the Department of Neuroradiology, Oberösterreichische Landesnervenklinik, Linz, Austria (F.F.); the Departments of Diagnostic Radiology (F.F., R.S.) and Medical Physics (C.F.), Friedrich-Alexander-University, Erlangen-Nürnberg, Germany; and the Department of Radiology, University of Regensburg (Germany) (P.H.).

Address reprint requests to Franz Fellner, MD, Department of Diagnostic Radiology, Friedrich-Alexander-University of Erlangen-Nürnberg, Maximiliansplatz 1, 91054 Erlangen, Germany.

AJNR 18:1617–1625, Oct 1997 0195-6108/97/1809–1617

sumed microvascular ischemic disease) were also examined.

Materials and Methods

Sixty-six patients, including 39 women and 27 men (mean age, 51 ± 17 years), with ischemic and neoplastic brain lesions were examined. The pathologic findings included astrocytoma (n = 12), meningioma (n = 8), glioblastoma (n = 5), metastasis (n = 3), oligodendroglioma (n = 2), oligoastrocytoma (n = 1), neurinoma (n = 1), medulloblastoma (n = 1), territorial infarct (n = 11), and presumed microvascular ischemic disease (n = 22). All studies were performed with a commercial 1.0-T whole-body MR unit, a maximal gradient field strength of 15 mT/m, a gradient rise time of 1.0 milliseconds, and a circularly polarized head coil. The following sequences proved to be optimal (in terms of image quality, contrast, section coverage, and measurement time) for routine clinical applications and were used in all patients. For conventional spin-echo sequences, parameters were 2200/13,80/1 (repetition time [TR]/echo time [TE]/excitations), a matrix size of 256 × 256, a readout bandwidth of 130/45 Hz per pixel, and a measurement time of 9 minutes 28 seconds. For fast spin-echo sequences, parameters were 2100/14,85 effective/2, an echo train length of 5, a matrix size of 252 × 256, a readout bandwidth of 130 Hz per pixel, and a measurement time of 3 minutes 35 seconds. For GRASE sequences, the parameters were 4000/110 effective/1, an echo train length of 21 (seven spin echoes, 14 gradient echoes), a matrix size of 252 × 256, a readout bandwidth of 195 Hz per pixel, and a measurement time of 52 seconds. Section parameters were identical for all sequences: 19 transverse sections, 6-mm section thickness (1.2-mm gap), and 220-mm field of view. The T2-weighted images of the three sequences were evaluated by visual and quantitative analysis.

Three independent observers evaluated the contrast characteristics of anatomic and pathologic structures using a score ranging from 1 to 5, where 1 indicated very low; 2, low; 3, moderate; 4, good; and 5, excellent contrast. The following anatomic structures were judged: gray matter, basal ganglia (especially the iron-containing red nucleus), vessels, and aqueduct to surrounding white matter. For pathologic structures, the contrast between the lesion and surrounding structures and the internal contrast of the lesions (tumors and territorial infarcts) were assessed using the same score, where 1 corresponded to very low and 5 to very high contrast. Furthermore, the markedness of artifacts (flow, chemical shift, and ringing) was evaluated using a score from 1 to 5, where 1 indicated lack of artifacts; 2, discrete; 3, moderate; 4, strong; and 5, enormous artifacts.

The visual evaluation of anatomic and pathologic structures, and of artifacts, was performed on separate workstations, which enabled the observers to window the images optimally in each case. To avoid direct comparisons, the images from the different sequences were read in a random distribution, whereby the observers were blinded to the image data.

Using operator-defined regions of interest, we measured the signal intensity of the following anatomic structures: gray matter, white matter, cerebrospinal fluid (CSF), fat, and the red nucleus. The same was done for pathologic structures: ischemic lesions and tumors, edema, and postoperative defects. Noise was assessed as the standard deviation of a large region free of artifacts outside the head (air). From these data, S/N values were calculated by using the following equation:

$$1) \qquad S/N = SI_{tissue}/noise$$

Furthermore, C/N ratios of different anatomic and pathologic structures were assessed using the following equation:

$$2) \qquad C/N = SI_{tissue1} - SI_{tissue2}/noise$$

C/N was defined such that positive values resulted for the conventional spin-echo technique.

Statistical analysis was applied to the results of the visual and quantitative image evaluations. For the visual evaluation, mean values of the scores given by the three observers were assessed for each criterion (visual and quantitative image analysis). Mean values and standard deviations were calculated for all patients and for each sequence. For statistical evaluation, Wilcoxon's test was performed. Differences with P less than .05 were regarded as statistically significant.

Results

Quantitative Image Analysis

The results of the quantitative evaluation of anatomic structures are shown in Table 1. S/N values of gray and white matter, fat, and the red nucleus were superior on the fast spin-echo images and inferior on the GRASE images relative to the conventional spin-echo images. S/N values of CSF were superior on fast spin-echo images and inferior on conventional spin-echo images relative to the GRASE images. All results were statistically significant.

C/N of gray–white matter showed the highest values on fast spin-echo images and the lowest values on GRASE images, with discrete differences among the three techniques. C/N of fat–white matter revealed considerably higher values on fast spin-echo images than on GRASE and conventional spin-echo images. For C/N of CSF–fat, significantly lower values were found on conventional spin-echo images than on fast spin-echo and GRASE images; for C/N of white matter–red nucleus, the lowest values were found on the GRASE images. All results were statistically significant, except for C/N of white

TABLE 1: S/N and C/N values of anatomic structures

	Technique			*P* Value		
	GRASE	FSE	SE	GRASE–SE	GRASE–FSE	FSE–SE
S/N white matter	23.1 ± 2.5	43.5 ± 4.7	38.9 ± 5.8	<.001	<.001	<.001
S/N gray matter	34.4 ± 4.9	57.5 ± 6.3	51.5 ± 8.2	<.001	<.001	<.001
S/N CSF	73.9 ± 5.7	83.4 ± 8.2	66.2 ± 9.8	<.001	<.001	<.001
S/N fat	41.0 ± 4.0	114.8 ± 17.0	46.5 ± 7.2	<.001	<.001	<.001
S/N red nucleus	24.7 ± 2.9	46.6 ± 4.5	39.5 ± 6.4	<.001	<.001	<.001
C/N gray–white matter	11.3 ± 4.5	14.0 ± 4.2	12.5 ± 4.7	<.05	<.001	<.001
C/N fat–white matter	17.9 ± 3.8	71.3 ± 15.4	7.6 ± 5.6	<.001	<.001	<.001
C/N CSF–fat	32.9 ± 3.6	−31.5 ± 14.0	19.6 ± 6.1	<.001	<.001	<.001
C/N white matter–red nucleus	3.70 ± 2.11	6.36 ± 2.41	6.55 ± 27	<.01	<.001	NS

Note.—Mean values (region-of-interest evaluation) and *P* values (Wilcoxon's test) are given. GRASE indicates gradient- and spin-echo; FSE, fast spin-echo; SE, spin-echo; and NS, not significant.

TABLE 2: S/N and C/N values of pathologic structures

	No.	Technique			*P* Value		
		GRASE	FSE	SE	GRASE–SE	GRASE–FSE	FSE–SE
S/N tumor	27	57.8 ± 15.6	88.8 ± 23.2	73.5 ± 22.4	<.001	<.001	<.001
S/N perifocal edema	17	64.9 ± 9.0	93.1 ± 11.1	81.7 ± 12.5	<.001	<.001	<.001
S/N postoperative defect	8	70.8 ± 7.4	84.9 ± 6.0	69.2 ± 7.4	NS	<.05	<.05
C/N tumor–CSF	27	−17.4 ± 16.7	3.81 ± 22.80	5.16 ± 19.7	<.001	<.001	<.001
C/N tumor–white matter	27	34.4 ± 17.5	44.7 ± 22.3	33.2 ± 20.3	NS	<.001	<.001
C/N perifocal edema–tumor	14	3.54 ± 13.3	3.77 ± 16.30	7.74 ± 16.70	<.05	NS	<.01
C/N perifocal edema–CSF	17	−9.84 ± 8.41	10.6 ± 7.6	15.4 ± 6.3	>.001	<.001	<.01
S/N presumed microvascular ischemic disease	22	38.6 ± 5.8	65.4 ± 8.3	57.5 ± 11.2	<.001	<.001	<.01
C/N CSF–presumed microvascular ischemic disease	22	33.9 ± 7.6	18.0 ± 7.2	7.00 ± 6.57	<.001	<.001	<.001
C/N presumed microvascular ischemic disease–white matter	22	15.1 ± 6.0	20.6 ± 6.6	18.4 ± 7.2	<.05	<.001	<.001
S/N territorial infarct	11	59.7 ± 12.7	82.3 ± 11.0	71.5 ± 8.2	<.001	<.01	<.01
C/N territorial infarct–CSF	11	−14.9 ± 10.9	0.35 ± 8.01	6.28 ± 7.74	<.01	<.01	<.01
C/N territorial infarct–white matter	11	37.2 ± 12.4	41.1 ± 10.0	35.0 ± 7.2	NS	<.05	<.01

Note—Mean values (region-of-interest evaluation) and *P* values (Wilcoxon's test) are given. GRASE indicates gradient- and spin-echo; FSE, fast spin-echo; SE, spin-echo; and NS, not significant.

matter–red nucleus as compared between the fast and conventional spin-echo sequences.

Results of the quantitative analysis of tumors appear in Table 2. S/N values of tumor and perifocal edema were significantly higher on fast spin-echo images and inferior on GRASE images as compared with conventional spin-echo images. S/N of postoperative defects had the highest values on the fast spin-echo images. There was no significant difference between the GRASE and conventional spin-echo techniques. For C/N values of tumor–CSF, the highest values were found on the GRASE images, with inversion of contrast characteristics relative to fast and conventional spin-echo images: on the GRASE images, CSF was brighter than tumor and edema, whereas on the fast and conventional spin-echo images, tumor and edema were brighter than CSF. C/N values of tumor–white matter were significantly increased on the fast spin-echo images, with no significant difference between GRASE and conventional spin-echo images. C/N values of perifocal edema–tumor and edema–CSF were significantly increased on the conventional spin-echo images (with inversion of contrast characteristics on GRASE images relative to the fast and conventional spin-echo images). For C/N of edema–tumor, the difference between the fast spin-echo and GRASE techniques was statistically significant.

Results of the quantitative analysis of ischemic lesions are shown in Table 2. S/N values of territorial infarcts and presumed microvascular ischemic lesions were superior on the fast spin-echo images and inferior on the

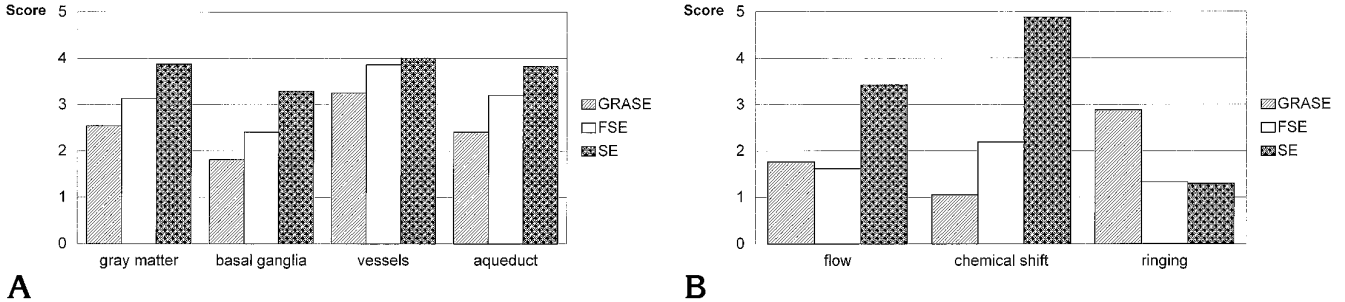

Fig 1. Contrast of anatomic structures and artifacts. Mean values (visual evaluation, score 1 to 5). *FSE* indicates fast spin-echo; *SE*, spin-echo.

A, Contrast of gray matter, basal ganglia, vessels, and aqueduct relative to surrounding white matter.

B, Flow artifacts, chemical-shift artifacts, and ringing artifacts.

GRASE images, with statistically significant differences.

C/N values of CSF–presumed microvascular ischemic lesions showed the highest values on the GRASE images, the lowest on the conventional spin-echo images. C/N values of presumed microvascular ischemic lesions–white matter were significantly higher on fast and conventional spin-echo images than on GRASE images. C/N of territorial infarcts–CSF had the highest values on GRASE images (with inverted contrast characteristics relative to fast and conventional spin-echo images) and the lowest on fast spin-echo images. C/N values of territorial infarcts–white matter showed the highest values on the fast spin-echo images. There was no significant difference between the GRASE and conventional spin-echo techniques.

Visual Image Analysis

Results of the visual evaluation of anatomic structures are shown in Figure 1A. Contrast of gray–white matter, basal ganglia, vessels, and aqueduct revealed the highest values on the conventional spin-echo images, the lowest on the GRASE images. The results were statistically significant, except for contrast of vessels on fast spin-echo images relative to that on conventional spin-echo images.

Results pertaining to artifacts are shown in Figure 1B. Flow artifacts were significantly reduced on fast spin-echo and GRASE images, without statistically significant differences in these fast techniques. Chemical-shift artifacts were considerably reduced on GRASE images as compared with conventional and fast spin-echo images, and each was statistically significant. Ringing artifacts were significantly pronounced on GRASE sequences as compared with conventional and fast spin-echo sequences (there was no significant difference between conventional and fast spin-echo sequences).

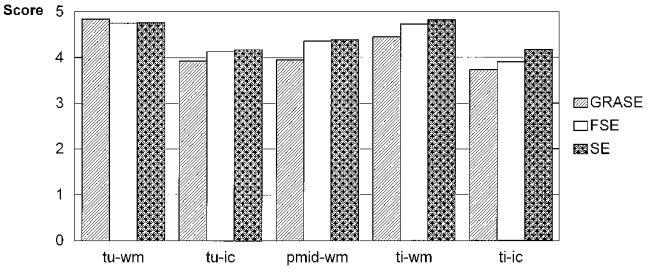

Fig 2. Contrast of tumors and ischemic lesions relative to surrounding structures, and internal contrast of lesions. Mean values (visual evaluation, score 1 to 5) (*tu* indicates tumor; *wm*, white matter; *ic*, internal contrast of tumors; *pmid*, presumed microvascular ischemic disease; *ti*, territorial infarct; *FSE*, fast spin-echo; and *SE*, spin-echo).

Results of the visual evaluation of pathologic structures are shown in Figure 2. There was no statistically significant difference among the three techniques in terms of the contrast between tumor and white matter or in depicting the internal contrast of tumors. The same results were found for the contrast of territorial infarcts–white matter and for the internal contrast of territorial infarcts. The contrast of presumed microvascular ischemic lesions was somewhat reduced on GRASE images (statistically significant).

Discussion

In the visual evaluation, the contrast characteristics of gray–white matter were superior on conventional spin-echo images and inferior on GRASE images, with only slight differences be-

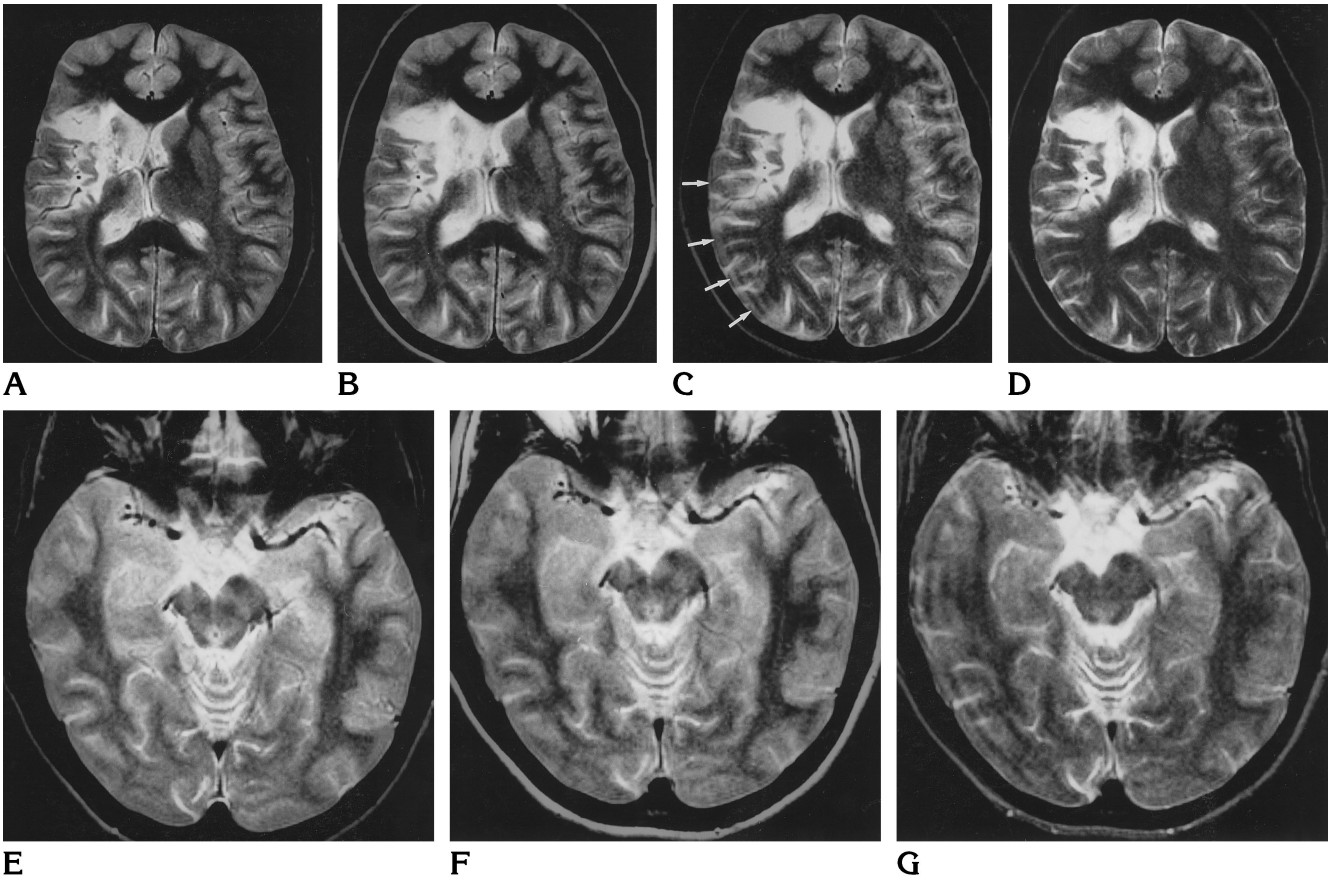

Fig 3. A 32-year-old patient with infarction in the territory of the right middle cerebral artery.

A, Conventional spin-echo; *B*, fast spin-echo; *C*, GRASE; *D*, GRASE; *E*, conventional spin-echo; *F*, fast spin-echo; *G*, GRASE.

Excellent contrast of gray to white matter is seen on conventional (*A*) and fast (*B*) spin-echo images, and is slightly diminished on GRASE image (*C*). Bright intensity of CSF seen on GRASE image is reduced by broader windowing in *D*, which thereby diminished contrast of gray to white matter, however. Note ringing artifacts (*arrows* in *C*). Relative to conventional (*E*) and fast (*F*) spin-echo images, contrast of the red nucleus, aqueduct, and vessels is reduced on GRASE image (*G*). Fat has high signal intensity on fast spin-echo image, and intermediate intensity on conventional spin-echo and GRASE images.

tween conventional and fast spin-echo images. The reduced contrast on the GRASE sequences can be partially explained by the high signal intensity of CSF, which requires broader windowing. This worsens the contrast of gray and white matter (Fig 3).

As opposed to the visual evaluation, the C/N values of gray–white matter were somewhat higher on the fast spin-echo images than on the conventional spin-echo images. This is the effect of higher signal gain on fast spin-echo sequences caused by the k-space order, with early echoes near its center (1, 2). This discrepancy between quantitative and visual image analysis has been observed on other fast spin-echo sequences (2). Therefore, another factor that leads to recognizable contrast deterioration in fast imaging techniques has to be postulated. In sequences with variable TEs, such as fast spin-echo and magnetization-prepared rapid gradient-echo techniques, there is a broadening of the so-called point spread function, depending on echo train length and k-space order, that results in blurring artifacts (16, 17). Blurring is enhanced with increasing echo train length. This phenomenon explains the reduced contrast of anatomic structures, such as gray and white matter, in fast spin-echo and GRASE techniques, especially with long echo train lengths. The reduced contrast of vessels and aqueduct on fast spin-echo images (Fig 4), and especially on GRASE compared with conventional spin-echo images, is also a result of the above-mentioned blurring. It is known that with conventional and fast spin-echo sequences, increasing T2 weighting reduces the flow void of

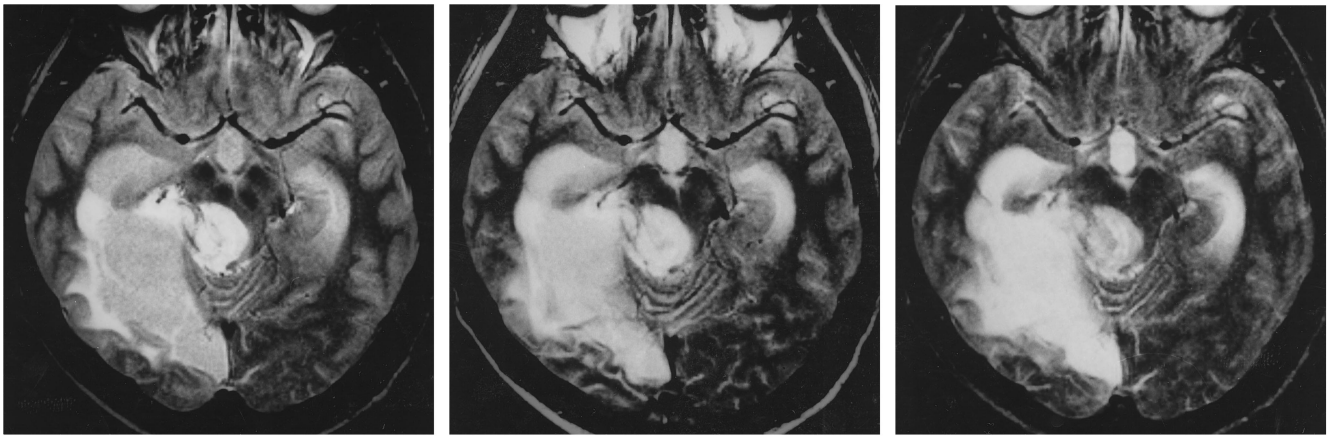

A B C

Fig 4. Postoperative control study in 41-year-old patient with astrocytoma (grade III). Best contrast of CSF-filled spaces, perifocal edema, and tumor is seen on conventional spin-echo sequence (*A*). Conventional (*A*) and fast (*B*) spin-echo images are nearly identical, only CSF is somewhat brighter on the latter. Inversion of contrast characteristics of CSF is seen on GRASE sequence (*C*), in which CSF is brighter than edema or tumor.

the aqueduct (1). Furthermore, blurring decreases the definition of the basal ganglia on fast imaging sequences (Fig 3). It is more difficult to delineate iron-containing nuclei with fast spin-echo and GRASE techniques than with conventional spin-echo techniques (1, 3, 18). This is an effect of the multiple, closely spaced 180° refocusing pulses that lead to higher signal gain, especially of susceptibility-sensitive objects. The same phenomenon is seen with GRASE techniques (15).

It is well known that fast spin-echo sequences display fat much brighter than conventional spin-echo techniques do (19–21) (Fig 3). Neighboring protons in hydrocarbon chains are linked by strong homonuclear interactions (J-coupling). Therefore, in a conventional spin-echo experiment, many fat spins fail to be refocused, resulting in intermediate to mild hyperintense signal intensity of fatty tissues on conventional spin-echo images. Multiple refocusing pulses within one TR interval, as in fast spin-echo sequences, are able to break these J-couplings. As early as 1966, Allerhand (22) postulated a correlation between the number of homonuclear coupled spins and echo spacing in a Carr-Purcell-Meiboom-Gill echo train. Increasing the number of refocusing pulses and decreasing echo spacing leads to destruction of J-couplings and, therefore, to increased fat intensity (19). These facts agree with the results of this study, in which fat had high intensity on fast spin-echo images and intermediate intensity on conventional spin-echo and GRASE images (Fig 3). There is a relatively wide echo spacing of the refocusing 180° pulses on GRASE images, because each spin-echo is surrounded by gradient echoes.

In the delineation of tumors, no significant differences were found among the three techniques in the visual evaluation (Figs 4 and 5). C/N values of tumor–CSF were higher on GRASE images, with inversion of contrast characteristics: although on fast and conventional spin-echo images most tumors are brighter than CSF, on GRASE images CSF is brighter owing to the heavy T2 contrast of the GRASE technique. Theoretically, tumor and CSF should be better differentiated on GRASE images because of the C/N values found in the region-of-interest evaluation. However, in practice, this is not the case. Owing to the high signal intensity of tumors, and especially of CSF, GRASE images must be displayed with broader windowing, which results in a deterioration in contrast characteristics of anatomic structures.

Perifocal edema–tumor and edema–CSF had the highest C/N values on the conventional spin-echo sequence. Thus, the conventional spin-echo sequence with its relatively short second echo time of 80 remains the best technique for differentiating CSF, edema, and tumor, closely followed by the fast spin-echo sequence (1) (Fig 4).

The visual delineation of territorial infarcts was similar for all techniques (Figs 3 and 6); that is, no lesion was missed. Presumed microvascular ischemic lesions, however, revealed a

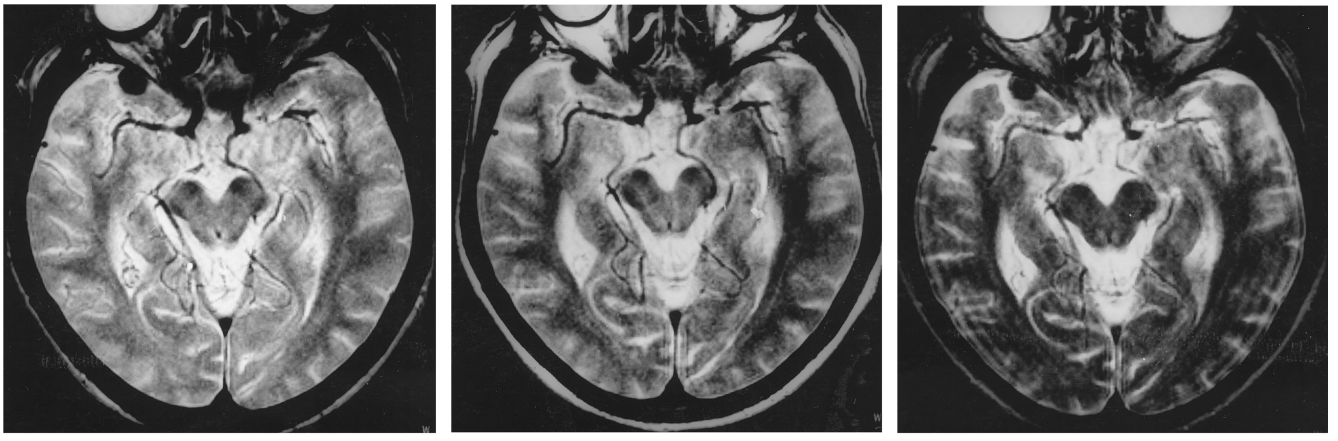

A B C

Fig 5. A 74-year-old patient with a small calcified meningioma of the sphenoidal wing on conventional spin-echo (*A*), fast spin-echo (*B*), and GRASE (*C*) images. Signal intensity of tumor is diminished on GRASE sequence.

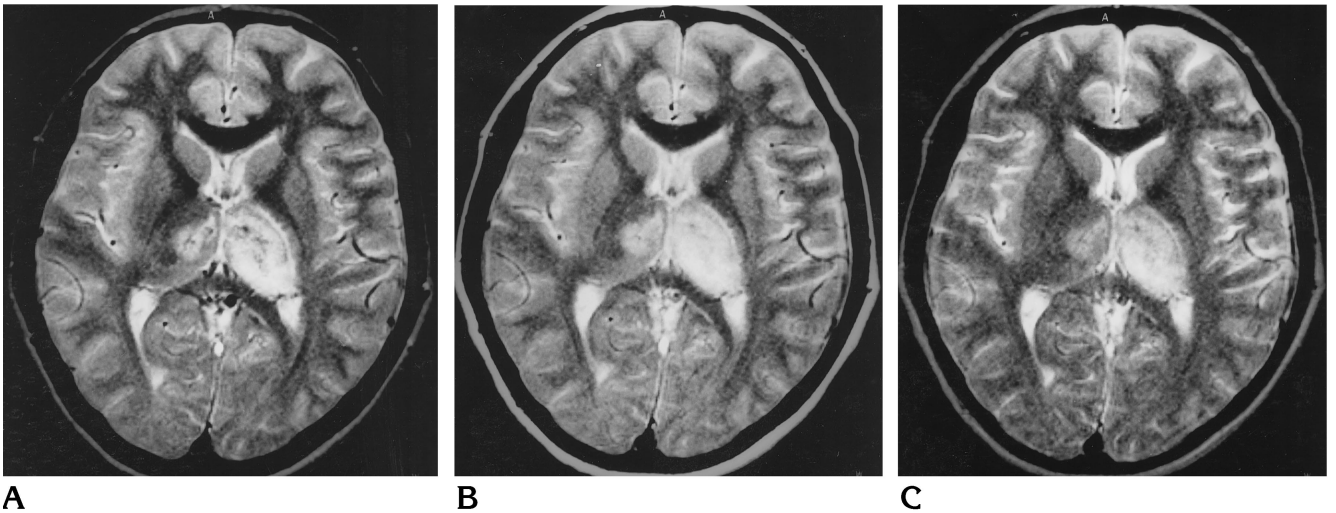

A B C

Fig 6. A 33-year-old patient with dural sinus thrombosis. Ischemic lesions in both thalami are adequately shown by conventional spin-echo (*A*), fast spin-echo (*B*), and GRASE (*C*) techniques.

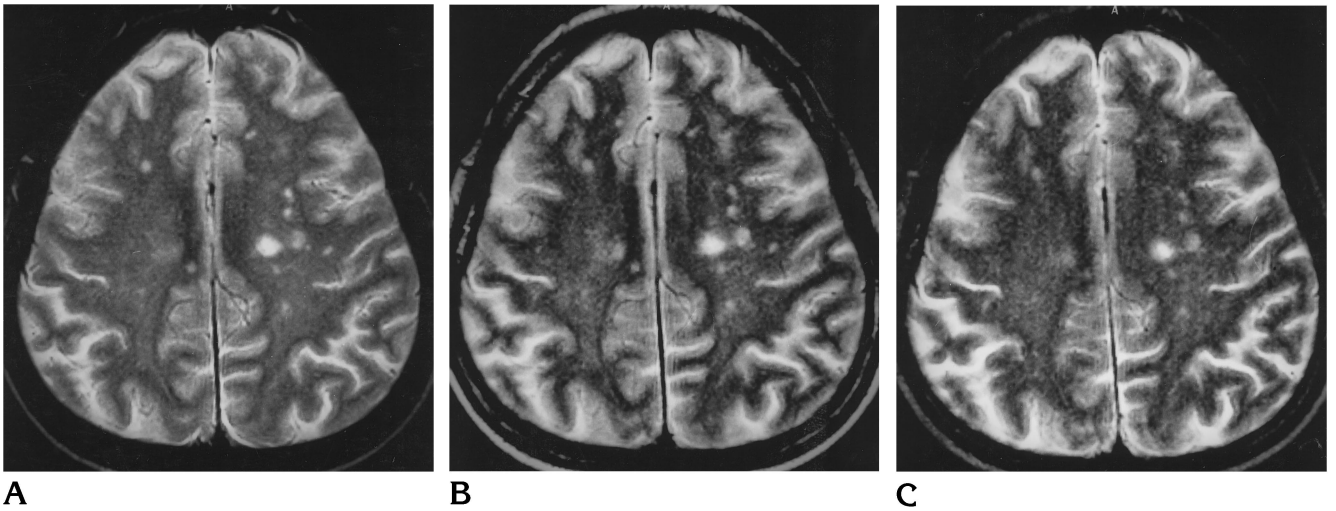

A B C

Fig 7. A 55-year-old patient with presumed microvascular ischemic (moyamoya) disease. Despite reduced contrast of small lesions on GRASE image (*C*), these lesions are clearly identified on conventional (*A*) and fast (*B*) spin-echo images. Blurring of the small defects is seen in phase-encoding direction on GRASE sequence.

slightly decreased delineation on GRASE images as compared with conventional and fast spin-echo images (Fig 7). Between conventional and fast spin-echo sequences, no significant differences were found. On GRASE images, blurring in the phase-encoding direction decreases visibility of small lesions located perpendicular to the phase-encoding direction (1, 16). At present, GRASE cannot match conventional and fast spin-echo techniques with respect to image quality and diagnostic accuracy. Currently, only acquisition of T2-weighted images with the GRASE technique is useful. Unless GRASE also provides proton density–weighted images (13), these images are only mildly T2-weighted, and CSF has isointense, not hypointense, signal intensity. However, low signal intensity of CSF on proton density–weighted images is important for delineation of small periventricular and subcortical lesions (1).

Flow artifacts are significantly reduced on fast spin-echo and GRASE images. Owing to the symmetric sequence design within a TR cycle, there is even echo rephasing, which reduces the total amount of flow artifacts (23). Reduction of flow artifacts may considerably improve conspicuity of small posterior fossa lesions (1). Chemical-shift artifacts were significantly reduced on the GRASE sequences as a result of the greater readout bandwidth. Most artifacts were found on conventional spin-echo images, owing to the narrow bandwidth. However, ringing artifacts were most pronounced on the GRASE sequences (Fig 3). This type of ghosting artifact is a relevant problem in single-shot echo-planar imaging sequences, which acquire all echoes after a single 180° pulse. Continuous increase of the phase-encoding gradient results in modulation of chemical shift and $T2^*$ in the phase-encoding direction (12). The same phenomenon is seen with the GRASE technique within a gradient-echo–spin-echo–gradient-echo group; however, it is less pronounced because there is a 180° refocusing pulse after each echo group (12).

In summary, fast sequences with spin-echo contrast characteristics have revolutionized MR imaging by significantly reducing measurement times while providing the same diagnostic accuracy as conventional spin-echo imaging. Therefore, the fast spin-echo sequences could replace conventional spin-echo techniques in MR imaging of the brain. The GRASE technique reduces measurement times even further relative to fast spin-echo imaging. At present, GRASE does not provide the image quality and contrast spectrum of conventional or fast spin-echo sequences; nevertheless, it might be useful for uncooperative patients whose conventional or fast spin-echo sequences show considerable motion artifacts.

In our study, fast spin-echo sequences were the best fast technique for acquisition of T2- and proton density–weighted MR images of the brain.

References

1. Fellner F, Schmitt R, Trenkler J, et al. True proton density and T2 weighted turbo spin-echo sequences for routine MRI of the brain. *Neuroradiology* 1994;36:591–597
2. Fellner C, Fellner F, Schmitt R, Helmberger T, Obletter N, Böhm-Jurkovic H. Turbo spin-echo sequences in magnetic resonance imaging of the brain: physics and applications. *MAGMA* 1994;2: 51–59
3. Jones KM, Mulkern RV, Mantello MT, et al. Brain hemorrhage: evaluation with fast spin-echo and conventional dual spin-echo images. *Radiology* 1992;182:53–58
4. Tice HM, Jones KM, Mulkern RV, et al. Fast spin-echo imaging of intracranial neoplasms. *J Comput Assist Tomogr* 1993;17:425–431
5. Hawnaur JM, Hutchinson CE, Isherwood I. Clinical evaluation of fast spin-echo sequences for cranial magnetic resonance imaging at 0.5 Tesla. *Br J Radiol* 1994;67:423–428
6. Jack CR Jr, Krecke KN, Luetmer PH, et al. Diagnosis of mesial temporal sclerosis with conventional versus fast spin-echo MR imaging. *Radiology* 1994;192:123–127
7. Prenger EC, Beckett WW, Kollias SS, Ball WS Jr. Comparison of T2-weighted spin-echo and fast spin-echo techniques in the evaluation of myelination. *J Magn Reson Imaging* 1994;4:179–184
8. Ahn SS, Mantello MT, Jones KM, et al. Rapid MR imaging of the pediatric brain using the fast spin-echo technique. *AJNR Am J Neuroradiol* 1992;13:1169–1177
9. Gass A, Barker GJ, MacManus D, et al. High resolution magnetic resonance imaging of the anterior visual pathway in patients with optic neuropathies using fast spin-echo and phased array local coils. *J Neurol Neurosurg Psychiatry* 1995;58:562–569
10. Oshio K, Feinberg DA. GRASE (gradient-and spin-echo) imaging: a novel fast MRI technique. *Magn Reson Med* 1991;20:344–349
11. Oshio K, Feinberg DA. Single shot GRASE imaging without fast gradients. *Magn Reson Med* 1992;26:355–360
12. Feinberg DA, Oshio K: GRASE (gradient- and spin-echo) MR imaging: a new fast clinical imaging technique. *Radiology* 1992; 181:597–602
13. Feinberg DA, Kiefer B, Litt AW. Dual contrast GRASE (gradient- and spin-echo) imaging using mixed bandwidth. *Magn Reson Med* 1994;31:461–464
14. Fellner F, Kiefer B, Trenkler J, Fellner C. Turbo-GSE: a rapid T2-weighted hybrid sequence for MR tomography with instruments of high-gradient field strength. *Fortschr Röntgenstr* 1994; 161:366–368
15. Fellner F, Schmitt R, Trenkler J, Fellner C, Böhm-Jurkovic H. Turbo gradient-spin-echo (GRASE): first clinical experiences with a fast T2-weighted sequence in MRI of the brain. *Eur J Radiol* 1995;19:171–176
16. Constable RT, Gore JC. The loss of small objects in variable TE

imaging: implications for FSE, RARE, and EPI. *Magn Reson Med* 1992;28:9–24
17. Fellner F, Holl K, Held P, Fellner C, Schmitt R, Böhm-Jurkovic H. A T1-weighted rapid three-dimensional gradient-echo technique (MP-RAGE) in preoperative MRI of intracranial tumors. *Neuroradiology* 1996;38:199–206
18. Melki PS, Mulkern RV, Panych LP. Comparing the FAISE method with conventional dual-echo sequences. *J Magn Reson Imaging* 1991;1:319–326
19. Constable RT, Anderson AW, Zhong J, Gore JC. Factors influencing contrast in fast spin-echo MR imaging. *Magn Reson Imaging* 1992;10:497–511
20. Constable RT, Smith RC, Gore JC. Coupled-spin fast spin-echo MR imaging. *J Magn Reson Imaging* 1993;3:547–552
21. Henkelman RM, Hardy PA, Bishop JE, Poon CS, Plewes DB. Why fat is bright in RARE and fast spin-echo imaging. *J Magn Reson Imaging* 1992;2:533–540
22. Allerhand A. Analysis of Carr-Purcell spin-echo NMR experiments on multiple spin systems, I: the effect of homonuclear coupling. *J Chem Phys* 1966;44:1–9
23. Fellner C, Geissler A, Held P, Strotzer M, Treibel W, Fellner F. Signal, contrast, and resolution in optimized PD– and T2-weighted turbo SE images of the knee. *J Comput Assist Tomogr* 1995;19:96–105